UCRL- 91355
PREPRINT

RESIDUAL LIMITATIONS OF THEORETICAL ATOMIC-ELECTRON BINDING ENERGIES

Mau Hsiung Chen
Lawrence Livermore National Laboratory

Bernd Crasemann
University of Oregon

Nils Mårtensson
University of Uppsala

Börje Johansson
University of Aarhus

This paper was prepared for submittal to
Physical Review A

August 1984

DISCLAIMER

Residual limitations of theoretical atomic-electron binding energies

Mau Hsiung Chen
Lawrence Livermore National Laboratory
P. O. Box 808, Livermore, California 94550

Bernd Crasemann
Department of Physics and Chemical Physics Institute
University of Oregon
Eugene, Oregon 97403

Nils Mårtensson
Institute of Physics
University of Uppsala
S-751 21 Uppsala, Sweden

Börje Johansson
Institute of Physics
University of Aarhus
DK-8000 Aarhus C, Denmark

August 1984

Abstract

Relativistic calculations of atomic-electron binding energies have been refined by using the relativistic LS-average scheme to treat open outer shells, by including self-energy corrections for shells up to 3p as well as 4s, and accounting for energy shifts caused by interaction with Coster-Kronig continua. The contributions of ground-state correlation were estimated from the pair energy calculated through nonrelativistic many-body theory. The need for a relativistic theory of correlations is noted. As in our previous work, the calculations include relaxation, the effect of finite nuclear size, Breit interaction, and quantum-electrodynamic corrections. Results are compared with binding energies measured on free atoms, and with solid-phase measurements on metals that have been corrected for solid-state shifts; these shifts were calculated under the assumption of complete screening, with the core-ionized site treated as a neutralized metallic impurity atom in the original metallic host. Discrepancies between experimental energies and relativistic independent-particle calculations including relaxation, QED, and finite-nuclear-size corrections are traced to correlation corrections, uncertainties in the self energy, and neglect of the effect of (super-)Coster-Kronig fluctuations.

I. INTRODUCTION

Atomic-electron binding energies are very interesting in several respects. A systematic comparison between theoretical and precisely measured atomic binding energies can provide sensitive tests of quantum-electrodynamic results and of calculations of electron-electron Coulomb correlation. In applications, the knowledge of binding energies is essential in the interpretation of Auger and photoelectron spectra and of a multitude of atomic and solid-state phenomena. Differences between the binding energies of atoms in the free state and in solids, and in various chemical environments, provide a useful probe of extraatomic effects that are as yet incompletely understood.

We have previously performed systematic relativistic calculations of atomic binding energies with Dirac-Hartree-Slater wave functions.[1,2] The calculations include the relaxation effect, finite-nuclear-size effect, Breit interaction, and quantum-electrodynamic corrections. The calculations were, however, carried out for the lowest j-j configuration; this has been found to lead to a spurious contribution to 2p and 3p fine-structure splittings of atoms with open outer shells. Furthermore, the correlation effect was completely ignored.

In order to correct for these deficiencies, new systematic calculations have been completed with the following improvements: (1) The relativistic LS-average scheme[3] was used to treat open outer shells. (2) The 3s, 3p, and 4s self-energy corrections obtained from the n^{-3} scaling rule and effective-charge approach were included in the calculations. (3) The energy shifts of 3s, 3p, 4s, 4p and 4d hole states caused by the interaction with Coster-Kronig continua were calculated on the basis of Fano's approach of configuration interaction with the continuum.[4] (4) The contributions of ground-state correlation were estimated from the pair energy calculated by nonrelativistic many-body theory.[5]

Experimental and semiempirical atomic-electron binding energies have been obtained from measurements on free atoms as well as solids. For deep levels, x-ray emission data were used. These data were combined with calculated metal-atom core-level shifts to derive semiempirical free-atom binding energies. The empirical information is critically compared with the new relativistic calculations.

II. THEORETICAL ATOMIC BINDING ENERGIES

Accurate binding-energy calculations must include the effects of relativity, both from single-electron and Breit interactions, as well as of finite nuclear size, relaxation, quantum electrodynamics, and correlations. At present, no unified theory exists that is capable of treating all these effects simultaneously. Thus, they are usually calculated additively.

We define the theoretical atomic-electron binding as

$$E_B = E_{ion}(N-1) - E_G(N). \qquad (1)$$

Here, $E_{ion}(N-1)$ and $E_G(N)$ are the total energies of the ion with N-1 electrons and the atom in its ground state with N electrons, respectively. In terms of the relativistic model, the binding energy can be decomposed as follows:

$$E_B = \mathcal{E}(DF) + E(RELAX) + E(MAGR) + E(LAMB) + E(CORR). \qquad (2)$$

Here, $\mathcal{E}(DF)$ is the eigenvalue from a Dirac-Fock calculation, equal to the result from Eq. (1) in the frozen-orbital approximation (Koopman's theorem); E(RELAX) is the relativistic relaxation energy. The third term in Eq. (2), E(MAGR), is the contribution from the magnetic and retardation corrections. The term E(LAMB) is the radiative correction including self energy and vacuum polarization, and the last term, E(CORR), is the correlation contribution to the

binding energy. We proceed to discuss these terms one by one.

A. Zero-order energy

The relativistic independent-particle models can be used to compute the zero-order wave functions and energies. The detailed theoretical treatment of the Dirac-Fock or Dirac-Hartree Slater approaches has been reviewed recently.[3,6] Here, we outline them only briefly.

We use the version of Liberman et al.[7] of the Dirac-Hartree-Slater (DHS) method with a modified finite-nucleus routine. The method employs a modified Kohn-Sham potential, which is essentially a Kohn-Sham potential with a tail correction, but formulated in a more consistent manner. A first-order correction to the local approximation is made in our calculations by computing the expectation of the total Hamiltonian with zeroth-order wave functions.[1,2,8] The effect of relaxation is taken into account by performing separate SCF calculations for ground and hole states. The binding energy is then found as the difference between these total energies (ΔSCF method). This zeroth-order DHS energy is equivalent to the sum of the first two terms in Eq. (2).

Even though j-j coupling is the natural scheme in relativistic calculations, LS coupling is more suitable for most atoms with open outer shells because the electrostatic interaction dominates here over the spin-orbit interaction. In the present calculations, we use the relativistic LS-average scheme[3] to treat open outer shells. The relativistic LS-averaged energy can be written as[3]

$$\langle E \rangle = \sum_a \langle q_a \rangle I_a + 1/2 \sum_{a,b,k} \langle q_a \rangle [C(abk)\, F^k(ab) + D(abk)\, G^k(ab)], \quad (3)$$

where

$$C(abk) = \begin{cases} [(q_B - 1)|(q_B^o - 1)]\, C^o(abk), & a,b \in B \\ [q_B|q_B^o]\, C^o(abk), & a \notin B,\ b \in B, \end{cases} \tag{4}$$

$$D(abk) = \begin{cases} [(q_B - 1)|(q_B^o - 1)]\, D^o(abk), & a,\ b \in B \\ [q_B|q_B^o]\, D^o(abk), & a \notin B,\ b \in B\ . \end{cases} \tag{5}$$

Here, the average occupation number $\langle q_a \rangle$ is

$$\langle q_a \rangle = [q_A|(4\ell_a + 2](2j_a + 1), \quad a \in A, \tag{6}$$

and the closed-shell angular factors $C^o(abk)$ and $D^o(abk)$ for closed shells b with quantum numbers $n\ell j$ are

$$C^o(abk) = \delta(k,0)\ (2j_b + 1)$$

and

$$D^o(abk) = -(2j_b + 1) \begin{pmatrix} j_a & k & j_b \\ -\frac{1}{2} & 0 & -\frac{1}{2} \end{pmatrix}^2 \Pi(\ell_a k \ell_b), \tag{7}$$

$$\Pi(\ell_a k \ell_b) = \begin{cases} 1 & \text{if } \ell_a + k + \ell_b = \text{even} \\ 0 & \text{otherwise} \end{cases} \tag{8}$$

The indices A,B,... and a,b,...represent major shells and subshells, respectively; q_B and q_B^o are the actual occupation number of shell B and the occupation number of a full shell B, respectively. The one-electron integral I_a and Slater integrals F^k and G^k are defined in Ref. 3.

The effect of finite nuclear size is quite important for the inner shells of heavy atoms. Our present theoretical data base of binding energies was calculated by using the Fermi nuclear charge distribution[2,6] for K- and L-level

energies, and a uniform charge distribution[1,6] for M and higher levels.

B. Magnetic and retardation contributions

The dynamic correction to the electrostatic Coulomb interaction, which takes account of the exchange of a single transverse photon, can be included through the use of the transverse operator or the Breit operator in first-order perturbation theory. In the Coulomb gauge, the transverse operator[9] is

$$H'_{Br} = - \frac{\vec{\alpha}_1 \cdot \vec{\alpha}_2}{r_{12}} + (\vec{\alpha}_1 \cdot \vec{\nabla}_1)(\vec{\alpha}_2 \cdot \vec{\nabla}_2) \frac{\cos(\omega r_{12})-1}{\omega^2 r_{12}} . \quad (9)$$

Here, ω is the wave number of the exchanged virtual photon, and $\alpha_{1,2}$ are the usual Dirac matrices. In the low-energy limit $\omega \to 0$, Eq. (9) reduces to the Breit operator

$$H_{Br} = - \frac{1}{2r_{12}} \left[(\vec{\alpha}_1 \cdot \vec{\alpha}_2) + \frac{(\vec{\alpha}_1 \cdot \vec{r}_{12})(\vec{\alpha}_2 \cdot \vec{r}_{12})}{r_{12}^2} \right]. \quad (10)$$

In the Lorentz gauge, the transverse operator can be expressed[9] as

$$H''_{Br} = - \frac{1}{r_{12}} [\vec{\alpha}_1 \cdot \vec{\alpha}_2 \cos\omega r_{12} + (1 - \cos\omega r_{12})]. \quad (11)$$

Detailed derivations of the matrix elements of the Breit and generalized Breit interactions have been provided by Grant[6] and by Mann and Johnson[9] in terms of a sum of products of angular factors and radial integrals. In the present work, we used the frequency-dependent Breit operator [Eq. (11)] for K and L binding energies, while the long-wavelength approximation to the Breit interaction [Eq. (10)] was employed for M and higher-shell energies. The spherically averaged Breit interaction energies[9] were calculated for atoms with open outer shells. The magnetic and retardation contributions to the binding

energies were thus included in results from the SCF method, which automatically takes account of relaxation as well.

C. Radiative corrections

There are two main radiative corrections to atomic electron energies: the self energy and vacuum polarization. The self-energy correction arises from the electron's interaction with the radiation field which leads to mean-square fluctuations in the electron position. The self-energy shift can be expressed, in atomic units, as

$$\Delta E = \left(\frac{1}{\alpha\pi}\right) \frac{(\alpha Z)^4}{n^3} F(\alpha Z). \tag{12}$$

Here, Z is the atomic number, α is the fine-structure constant, and n is the principal quantum number. In the present work, the self-energy corrections for K and L levels were calculated from point-Coulomb values[10] with an effective-charge screening procedure.[2] For M_1, $M_{2,3}$, and N_1 levels, the self-energy corrections were estimated with the use of the n^{-3} scaling rule [Eq. (12)] and effective-charge approach.

The second important radiative correction is the vacuum polarization, which arises because the effective potential seen by the electron is modified by the polarized vacuum charge distribution due to the virtual electron-positron pairs. Here we have used the Uehling potential and higher-order terms from Huang[11] in first-order perturbation theory to calculate the vacuum-polarization correction to the binding energies in the ΔSCF scheme.[1,2]

D. Correlation effects

The effects of correlation on atomic binding energies can be quite important in some cases. Correlation effects are usually estimated from

nonrelativistic theory because no suitable relativistic correlation theory exists. The nonrelativistic treatment is primarily suited for light atoms, hence detailed information on correlation contributions to the binding energies of heavier elements is lacking as yet.

In principle, one should find the correlation contribution to the binding energies by calculating the total correlation energies for ground and hole states and taking the difference. This, however, is a very expensive proposition, and a more tractable procedure needs to be chosen. In our present binding-energy calculations, the correlation energies of the passive electrons from ground and hole states are assumed to cancel each other completely. We therefore only need to concern ourselves with two important correlation contributions to the binding energy, viz., the ground-state correlation correction and the energy shift due to Coster-Kronig and super-Coster-Kronig fluctuations of the hole state.

The ground-state correlation correction arises because of the broken pairs in the hole state. This effect always increases the binding energy, since all pair energies are negative and there are more pairs in the ground state than in the hole state. The ground-state correlation effect is the dominant correlation contribution to the binding energy for an outermost shell, and for inner shells with orbital angular momentum $\ell = n-1$, where n is the principal quantum number. In this work, the ground-state correlation correction $E_{gc}(a)$ is evaluated as a sum of pair energies that survive after cancellation between ground and hole states:[12]

$$E_{gc}(a) = \frac{1}{2(2\ell_a+1)} \sum_b E^o_{vv'}(a,b) + \frac{1}{2\ell_a+1} E^o_{vv'}(a,a), \qquad (13)$$

where $E_{vv'}{}^o(a,b)$, the total pair energy between two closed shells, is

$$E^o_{vv'}(a,b) = \sum_{L,S} (2S+1)(2L+1)\, \mathcal{E}(n_a\ell_a, n_b\ell_b; SL), \qquad (14)$$

with $\mathcal{E}(n_a\ell_a, n_b\ell_b;SL)$ being the symmetry-adapted pair energy.

A search of the literature for atomic correlation energies produces results for only some ten elements with $Z \leqslant 30$, all from nonrelativistic correlation theories.[13-18] From these pair energies and Eq. (13), we have estimated the ground-state correlation corrections to the binding energies of these atoms; some of the results are listed in Table I.

Another important correlation contribution to the binding energy is produced by dynamic relaxation processes in which the core hole fluctuates to intermediate levels of the Coster-Kronig or super-Coster-Kronig type, in addition to creating electron-hole pair excitation.[12,19] These effects are important for inner-shell hole states that can decay by Coster-Kronig or super-Coster-Kronig transitions (e.g., 2s, 3s, 3p, 4s, and 4p hole states). For transitions that are energetically impossible, these effects always reduce the binding energies; they can be estimated by finite configuration-interaction or MCHF methods.

When the hole state is embedded in the (super-) Coster-Kronig continua, we can use Fano's approach[4] of configuration interaction with the continuum to calculate the energy shift. Neglecting the effect of channel coupling, the energy shift due to the interaction with the continua can be calculated by solving the following equation[4,20,21] for E:

$$E - E_\phi = \sum_{\lambda=1}^{N} \mathcal{P} \int \frac{|\langle \Psi_{\lambda\varepsilon} | \sum_{i<j} r_{ij}^{-1} | \Phi \rangle|^2}{E - E_\lambda - \varepsilon} \, d\varepsilon , \qquad (15)$$

Here, E_ϕ and E_λ are the threshold energies of the single hole state and doubly ionized Auger continuum, respectively. The symbol $\mathcal{P}$ indicates the principal value fo the integral. The Auger matrix element for channel λ is evaluated

with the aid of a general relativistic program.[22] This correction has been found to remove the discrepancy between the relativistic ΔSCF result and experiments, for the 2s level. [21] In Table II, we list the energy shifts produced by the (super) Coster-Kronig fluctuations for 3s, 3p, 4s, 4p and 4d levels. For completeness, the results for the 2s level from Ref. 21 are also included in Table II.

III. DERIVATION OF EXPERIMENTAL BINDING ENERGIES

For the present systematic comparison between experimental and calculated binding energies, experimental data for a large number of core levels are required. Free-atom experimental energies are, however, available for only a limited number of atoms, mainly for the rare gases and for the non-transition metals. These results are furthermore limited to only a few of the core levels. The available data have been measured by a variety of experimental techniques,[23,24] such as photoelectron spectroscopy,[25-29] Auger-electron spectroscopy,[30,31] photoabsorption spectroscopy,[32] and x-ray emission spectroscopy.[33,34] To extend these results to the remaining core levels for the same elements we have used binding-energy differences derived from solid-phase measurements, either by photoelectron spectroscopy[35-39] or by x-ray emission spectroscopy. The main source for x-ray emission values is the tabulation of Bearden,[40] but in some cases we have also been able to use more recent values.[41] The accuracy of the tabulated x-ray energies was checked by studying systematic trends; obviously wrong values were excluded from the compilation.

In order to make the comparison more complete we have also included a large number of metallic elements, for which only solid-phase measurements have been performed.[23] For these cases we have used calculated free-atom to metal core-level shifts to derive free-atom binding energies.[24] It has been shown[24] that these shifts can be calculated with considerable accuracy, whence the indirectly

derived "experimental" values can be expected to be not much less accurate than the directly measured ones. The shifts were calculated within the complete screening picture, and the core-ionized site was treated as a neutralized metallic impurity atom in the original metallic host.[24] This model has been successfully applied to many other situations as well, such as the Auger process[42] and various satellite processes involving higher-ionized states.[43] The model furthermore leads to a good description of chemical shifts in metallic systems, such as alloy chemical shifts[44] and surface core-level shifts,[45] which also indicates that the model accounts well for the fundamental properties of the metallic influence.

IV. COMPARISON BETWEEN THEORY AND EXPERIMENT

The zeroth-order energies from our corrected DHS calculations are found to agree with the energies calculated from a Dirac-Fock model to better than 0.5 eV in all cases.[46] This establishes the reliability of our corrected DHS method.

Fine-structure splittings between $2p_{1/2}$ and $2p_{3/2}$ energy levels from theory and experiment are compared in Fig. 1. Open outer shells cannot adequately be treated in j-j coupling; a spurious contribution results that causes calculations for the lowest j-j configuration of an atom[1] to overestimate the fine-structure splitting if the atom has an open outer shell. On the other hand, theoretical energy splittings calculated in the relativistic LS average scheme (as in the present work) can agree well with measurements.

In Fig. 1 we display results from a DHS calculation for the lowest j-j configuration, including Breit interaction [Eq. (10)], as well as results from a DHS calculation in which the relativistic LS average scheme was employed and the transverse operator of Eq. (11) was used; we also show results from DF

eigenvalues.[47] Self-energy corrections for both L_2 and L_3 levels are included in the two DHS SCF calculations.

Several observations can be made with regard to the comparison in Fig. 1:

(i) The effect of the Breit interaction on the 2p fine-structure splittings is quite significant, even for low-Z elements. It is for this reason that DF eigenvalues lead to excessive splittings.

(ii) Because j-j coupling is inadequate for treating open outer shells, leading to a spurious contribution, theoretical results calculated for the lowest j-j configuration overestimate the splittings for atoms with open 3p, 3d, 4p, and 4d outer shells. A similar effect can be noted in other fine-structure splittings.

(iii) The error caused by use of the long-wavelength approximation for the Breit interaction becomes significant for the 2p fine structure above Z=40.

(iv) Theoretical results calculated in the relativistic LS average scheme with the frequency-dependent Breit interaction agree quite well with experiments. The remaining discrepancy for the 3d transition series has been shown to be due to exchange splitting which was not included in the present calculations.[48]

The self-energy corrections for 3s, 3p, and 4s levels of heavy elements ($Z \gtrsim 70$) from the n^{-3} scaling rule are found to be not negligible. For the 3s level, the self-energy correction is as large as $\sim$10 eV for $_{92}U$. The self-energy correction drastically reduces the discrepancies between theory and experiment.

Theoretical and experimental binding energies are compared in Figs. 2-6. We proceed to discuss the implications of these systematic comparisons for each level.

a. <u>1s level</u>

It is apparent from Fig. 2 that binding energies calculated in the

relativistic independent-particle model, including relaxation effects and QED corrections, are smaller than measured energies by 1-2 eV for $Z \lesssim 56$, and by 4-8 eV for $70 \lesssim Z \lesssim 92$. The correlation effect on 1s binding energies is dominated by the ground-state correlation correction; the interactions with double-hole continua for 1s hole states are all of the Auger type rather than Coster-Kronig, hence they are negligible.[21] The ground-state correlation corrections for $Z \lesssim 30$ were estimated from Table I; above Z=30, a constant correction of 1.7 eV (as calculated for $_{30}$Zn) was used throughout. It is clear from Fig. 2 that the ground-state correlation correction accounts for the entire discrepancy between relativistic independent-particle-model results and experimental binding energies up to $Z \approx 56$. Above Z=70, the ground-state correlation correction improves the agreement between theory and experiment but residual errors of ~3 eV still remain. This persistent discrepancy is probably due to errors in screening and relaxation corrections to the self energy. It should also be noted that we overestimate the ground-state correlation correction for low-Z atoms because of the frozen-orbital approximation [Eq. (13)]. Separate correlation-energy calculations for the neutral Ne atom and for the 1s hole state of Ne have shown that relaxation causes a reduction in the ground-state correlation correction, from 1.43 eV to 0.60 eV.[49]

b. 2s levels

For $Z \lesssim 5$, the discrepancy between predictions from the independent-particle model and measured 2s binding energies is removed when the ground-state correlation correction is included. For $Z \gtrsim 10$, the ground-state correlation correction increases the binding energies by ~1.5 eV. In the range $10 \lesssim Z \lesssim 20$, the super-Coster-Kronig fluctuations $[2s] \leftrightarrow [2p^2]nd$ reduce the binding energies by ~2 eV. For $30 \lesssim Z \lesssim 85$, the Coster-Kronig fluctuations $[2s] \leftrightarrow [2p3d]nf$ reduce the binding energies by 3-6 eV. After including correlation effects, we find

good agreement between calculated and measured 2s binding energies for $Z \lesssim 80$ (Fig. 2), but above Z=80, theory still overestimates the binding energies by ~7 eV. This residual discrepancy can be attributed to the uncertainty in self-energy and correlation corrections.

c. 2p levels

Auger fluctuations have only a very small effect on 2p binding energies.[21] The ground-state correlation correction is of the order of 2.5 eV. For Z=10, with 2p being the outermost shell, the relaxation effect on the ground-state correlation correction can be expected to be quite small, and indeed there is good agreement between theoretical and experimental binding energies (Fig. 3). But for $11 \lesssim Z \lesssim 56$, the ground-state correlation correction is too large by 1-2 eV due to the neglect of relaxation. The large errors in the binding energies of the 3d transition metals are partly due to the exchange splittings.

d. 3s levels

For $18 \lesssim Z \lesssim 20$, the super-Coster-Kronig fluctuations $[3s] \leftrightarrow [3p^2]nd$ reduce the 3s binding energies by ~6.5 eV. For $30 \lesssim Z \lesssim 54$, the binding energies are reduced by ~3-5 eV due to $[3s] \leftrightarrow [3p3d]nf$ super-Coster-Kronig fluctuations. A reduction of 3s binding energies by 7-8 eV occurs for atoms with atomic numbers above $Z \tilde{=} 70$ because of $[3s] \leftrightarrow [3p3d]nf$, $[3s] \leftrightarrow [3p4d]nf$, and $[3s] \leftrightarrow [3p4f]ng$ fluctuations. Once correlation effects are included, good agreement between theory and experiment is attained for $Z \lesssim 54$, but some discrepancies remain for $Z \gtrsim 70$ (Fig. 3), due to the uncertainty of the self-energy and correlation corrections.

e. 3p levels

For atomic number below $Z \tilde{=} 20$, 3p binding energies calculated from the independent-particle model are ~1 eV smaller than measurements, due to the neglect of ground-state correlation. Above $Z \tilde{=} 23$, the calculated energies are larger than measured binding energies due to the neglect of Coster-Kronig

fluctuations, the dominant mechanisms being $[3p] \leftrightarrow [3d^2]nf$ for $Z \lesssim 54$; $[3p] \leftrightarrow [3d^2]nf$ and $[3p] \leftrightarrow [3d4f]ng$ for $Z \gtrsim 70$ (Fig. 4).

f. 3d levels

Below Z=54, theoretical 3d binding energies from the independent-particle DHS model are smaller than measured energies (Fig. 4). Inclusion of the ground-state correlation correction for Cu and Zn (~3 eV) brings theory and experiment into agreement for these two elements (Fig. 4). Between Z=29 and Z=54, the discrepancy between IPM DHS results and measurements decreases gradually from 3.5 eV to 0.6 eV. This behavior could be caused by the relaxation effect on ground-state corerlation. There are no theoretical calculations of ground-state correlation in this range of atomic numbers to indicate whether this can account for the difference. For heavier atoms, no particular trend is discernible.

g. 4s and 4p levels

The ground-state correlation correction takes account of the difference between theoretical DHS IPM and measured 4s binding energies below Z=30 and 4p binding energies below $Z \tilde{=} 40$ (Figs. 5 and 6). For heavier elements, the IPM calculations consistently overestimate these binding energies due to the neglect of Coster-Kronig fluctuations. The most important of these fluctuations are $[4s] \leftrightarrow [4d4p]nf$ for $Z \tilde{=} 54$, $[4s] \leftrightarrow [4p4f]ng$ for $Z \tilde{=} 80$, $[4p] \leftrightarrow [4d^2]nf$ for $Z \tilde{=} 54$, and $[4p] \leftrightarrow [4d^2]nf$ and $[4p] \leftrightarrow [4d4f]ng$ for $Z \gtrsim 70$. Fair agreement between theory and experiment is obtained once correlation effects are included.

h. 4d and 4f levels

For 4d levels in atoms with $Z \lesssim 56$ and 4f levels in atoms below $Z \tilde{=} 83$, the relativistic independent-particle model underestimates the binding energies due to the neglect of ground-state correlation effects (Figs. 5, 6). As for the 3d level, these discrepancies become less with increasing atomic number. For the 4d levels, the super-Coster-Kronig fluctuations $[4d] \leftrightarrow [4f^2]ng$ becomes quite

important in atoms with $Z \gtrsim 70$. This correlation effect reduces the 4d binding energies for $Z \gtrsim 70$ by 3-4 eV.

V. CONCLUSION

The effects of relativity, relaxation, finite nuclear size, and QED corrections are all found to be important in the calculation of inner-shell binding energies. A unified relativistic theory of correlations would be most useful, but in the absence of such a theory the additive approach described in Sec. II turns out to be adequate.

Binding energies for outermost shells and shells with $\ell = n-1$ calculated from the relativistic independent-particle model including relaxation, QED, and finite-nuclear-size corrections are smaller than measured energies, due to neglect of the ground-state correlation correction. For 1s, 2p, and 3d levels of atoms with atomic numbers up to Z=60, as well as for the outermost shells, the discrepancy is ~ 3 eV; for 4f levels it can reach 5 eV. The discrepancy between theory and experiment is larger for the 1s levels of heavy elements, because of the uncertainty in the self-energy correction and neglect of the ground-state correlation correction. For inner-shell 2s, 3s, 3p, 4s, and 4p hole states, the relativistic independent-particle theory overestimates binding energies by as much as 13 eV, mostly due to neglect of the effect of (super-) Coster-Kronig fluctuations. Once the correlation correction to the theoretical binding energies is included, agreement between theory and experiment becomes better than ~ 3 eV, except for 2s and 3s levels of heavy elements, for which agreement is attained within ~ 6 eV.

ACKNOWLEDGMENTS

This work was performed in part under the auspices of the U. S. Department of Energy by the Lawrence Livermore National Laboratory under Contract No. W-7405-ENG-48. At the University of Oregon, this work was supported in part by the Advanced Research Projects Agency of the Department of Defense, monitored by the Air Force Office of Scientific Research under Contract No. F49620-84-C-0039.

References

1. K.-N. Huang, M. Aoyagi, M. H. Chen, B. Crasemann, and H. Mark, At. Data Nucl. Data Tables 18, 243 (1976).
2. M. H. Chen, B. Crasemann, M. Aoyagi, K.-N. Huang, and H. Mark, At. Data Nucl. Data Tables 26, 561 (1981).
3. I. Lindgren and A. Rosén, Case Studies in Atomic Physics 4, 93 (1974).
4. U. Fano, Phys. Rev. 124, 1866 (1961).
5. O. Sinanoğlu and K. A. Brueckner, Three Approaches to Electron Correlation in Atoms (Yale University Press, New Haven, 1970).
6. I. P. Grant, Adv. Phys. 19, 747 (1970).
7. D. A. Liberman, D. T. Cromer, and J. T. Waber, Comp. Phys. Commun. 2, 107 (1971).
8. A. Rosén and I. Lindgren, Phys. Rev. 176, 114 (1968).
9. J. B. Mann and W. R. Johnson, Phys. Rev. A 4, 41 (1971).
10. P. J. Mohr, Ann. Phys. (N.Y.) 88, 52 (1974); Phys. Rev. Lett. 34, 1050 (1975); Phys. Rev. A 26, 2338 (1982).
11. K.-N. Huang, Phys. Rev. A 14, 1311 (1976).
12. D. R. Beck, and C. A. Nicolaides, in Excited States in Quantum Chemistry, edited by C. A. Nicolaides and D. R. Beck (Reidel, Dordrecht, 1978).
13. H. P. Kelley, Phys. Rev. 136B, 896 (1964).
14. R. K. Nesbet, Phys. Rev. 155, 56 (1967); 175, 2 (1968).
15. I. Öksüz, and O. Sinanoğlu, Phys. Rev. 181, 42 (1969); 181, 54 (1969).
16. E. R. Cooper, Jr., and H. P. Kelly, Phys. Rev. A 7, 38 (1973).
17. K. Jankowski, P. Malinowski, and M. Polasik, J. Phys. B 12, 3157 (1979); 13, 3909 (1979); J. Chem Phys. 76, 448 (1982).
18. K. Jankowski and P. Malinowski, Phys. Rev. A 21, 45 (1980).

19. M. Ohno and G. Wendin, J. Phys. B 11, 1557 (1979); 12, 1305 (1979).

20. G. Howat, T. Åberg, and O. Goscinski, J. Phys. B 11, 1575 (1978).

21. M. H. Chen, B. Crasemann, and H. Mark, Phys. Rev. A 24, 1158 (1981).

22. M. H. Chen, E. Laiman, B. Crasemann, M. Aoyagi, and H. Mark, Phys. Rev. A 19, 2253 (1979).

23. An extensive compilation of core ionization energies will be presented elsewhere. For the sake of brevity, only selected references are indicated here. For instance, many references concerning metallic atoms are contained in Ref. 24 and are not repeated here.

24. B. Johansson and N. Mårtensson, Phys. Rev. B 21, 4427 (1980).

25. K. Siegbahn, C. Nordling, G. Johansson, J. Hedman, P. F. Hedén, K. Hamrin, U. Gelius, T. Bergmark, L. O. Werme, R. Manne, and Y. Baer, ESCA Applied to Free Molecules (North-Holland, Amsterdam, 1969).

26. Topics in Applied Physics 26 and 27, Photoemission in Solids, edited by M. Cardona and L. Ley (Springer, Berlin, 1978).

27. S. Svensson, N. Mårtensson, E. Basilier, P.-Å. Malmquist, U. Gelius, and K. Siegbahn, Phys. Scripta 14, 141 (1976).

28. T. D. Thomas and R. W. Shaw, Jr., J. Electron Spectrosc. Rel. Phen. 5, 1081 (1974).

29. J. S. H. Q. Perera, D. C. Frost, C. A. McDowell, C. S. Ewig, R. J. Key, and M. S. Banna, J. Chem. Phys. 77, 3308 (1982).

30. S. Othani, H. Nishimura, H. Suzuki, and K. Wakiya, Phys. Rev. Lett. 36, 863 (1976).

31. S. Aksela, M. Harkoma, and H. Aksela, Phys. Rev. A 29, 2915 (1984).

32. M. Breinig, M. H. Chen, G. E. Ice, F. Parente, and B. Crasemann, Phys. Rev. A 22, 520 (1980).

33. H. Ågren, J. Nordgren, L. Selander, C. Nordling, and K. Siegbahn, J. Electron Spectrosc. Rel. Phen. 14, 27 (1978).

34. J. Nordgren, H. Ågren, C. Nordling, and K. Siegbahn, Phys. Scripta 19, 5 (1979).

35. For the solid-phase binding energies we have mainly used Refs. 26 and 36-39.

36. A. Lebugle, U. Axelsson, R. Nyholm, and N. Mårtensson, Phys. Scripta 23, 825 (1981).

37. R. Nyholm and N. Mårtensson, Solid State Commun. 40, 311 (1981).

38. R. Nyholm, A. Berndtsson, and N. Mårtensson, J. Phys. C 13, L1091 (1980).

39. J. C. Fuggle and N. Mårtensson, J. Electron Spectrosc. Rel. Phen. 21, 275 (1980).

40. J. A. Bearden, Revs. Mod. Phys. 39, 78 (1967).

41. E. G. Kessler, Jr., R. D. Deslattes, D. Girard, W. Schwitz, L. Jacobs, and O. Renner, Phys. Rev. A 26, 2696 (1982).

42. N. Mårtensson, P. Hedegård, and B. Johansson, Phys. Scripta, 29, 154 (1984).

43. N. Mårtensson and B. Johansson, Phys. Rev. B 28, 3733 (1983).

44. P. Steiner, S. Hüfner, N. Mårtensson, and B. Johansson, Solid State Commun. 37, 73 (1981).

45. B. Johansson and N. Mårtensson, Helv. Phys. Acta, 56, 405 (1983).

46. M. H. Chen, in Atomic Inner-Shell Physics, edited by B. Crasemann (Plenum, New York, in press), and unpublished.

47. J. P. Desclaux, At. Data Nucl. Data Tables 12, 311 (1973).

48. C. S. Fadley and D. A. Shirley, Phys. Rev. A 2, 1109 (1970).

49. C. M. Moser, R. K. Nesbet, and G. Verhagen, Chem. Phys. Lett. 12, 230 (1971).

TABLE I. Ground-state correlation corrections to the binding energy (in eV).

Element	Level						
	1s	2s	2p	3s	3p	3d	4s
$_{4}Be$	1.21	1.26					
$_{10}Ne$	1.50	1.60					
$_{12}Mg$	1.53	1.50	2.54	1.01			
$_{18}Ar$	1.57	1.35	2.62	1.49	2.15		
$_{30}Zn$	1.70	1.71	3.09	2.13	2.12	3.27	1.59

TABLE II. Level-energy shift (in eV) produced by (super-)Coster-Kronig fluctuations.

Atomic number	Level					
Z	2s	3s	3p	4s	4p	4d
12	-2.4					
18	-2.2	-6.3				
19		-6.6[a]				
20	-2.1					
30	-3.3	-4.5	-3.2			
36	-5.0	-4.5	-4.7	-5.2		
40	-4.8					
45	-3.7					
46				-6.4		
47	-4.4	-3.2	-3.0			
54		-3.5	-2.7	-9.8	-11.3	
55					-11[a]	
56				-7.8	-10.5	
70		-7.9	-3.0	-10.1	-8.4	
74		-8.1	-3.5	-10.2	-8.3	-4.0
78	-6.2					
80	-4.2	-8.4	-4.7	-10.3	-8.2	-2.9
85	-3.2					
90	-2.2					
92	-1.7	-6.9	-5.8	-9.5	-9.9	-4.4
95			-6.1			

[a]From Ref. 12

Figure Captions

Fig. 1. Differences between calculated and measured spin-orbit splittings between $2p_{1/2}$ and $2p_{3/2}$ hole-state energies, in eV, as functions of atomic number Z. Theoretical energies were calculated in terms of the lowest j-j configuration with the long-wavelength approximation for the Breit interaction (solid circles linked by broken curve) and from the relativistic LS average with the frequency-dependent form of the Breit interaction (solid circles linked by solid curve). For comparison, the splittings from Dirac-Fock eigenvalues are also shown (triangles linked by solid curve).

Fig. 2. Differences between measured and calculated K (1s) and L_1 (2s) electron binding energies (in eV), as functions of atomic number Z. Theoretical energies were calculated from the relativistic independent-particle model alone (DHS-IPM), with inclusion of ground-state correlation (DHS-GC), and with inclusion of ground state correlation as well as (super-) Coster-Kronig fluctuations (DHS-GC-CK). Energies are plotted as functions of atomic number Z. Curves are drawn as guides for the eye only.

Fig. 3. Differences between measured and calculated L_3 ($2p_{3/2}$) and M_1 (3s) electron binding energies (in eV), as functions of atomic number Z. Theoretical energies were calculated as explained in the caption of Fig. 2. Curves are drawn merely to guide the eye.

Fig. 4. Differences between measured and calculated M_3 ($3p_{3/2}$) and M_5 ($3d_{5/2}$) electron binding energies (in eV), as functions of atomic number Z. Theoretical energies were calculated as explained in the caption of Fig. 2. Curves linking the calculated points are intended as guides for the eye only.

Fig. 5. Differences between measured and calculated N_1 (4s) and N_5 ($4d_{5/2}$) electron binding energies (in eV), as functions of atomic number Z. Theoretical energies were calculated as explained in the caption of Fig. 2. Curves are

drawn as guides for the eye.

Fig. 6. Differences between measured and calculated N_3 ($4p_{3/2}$) and N_7 ($4f_{7/2}$) electron binding energies (in eV), as functions of atomic number Z. Theoretical energies were calculated as explained in the caption of Fig. 2. Curves linking calculated points are drawn only as guides for the eye.

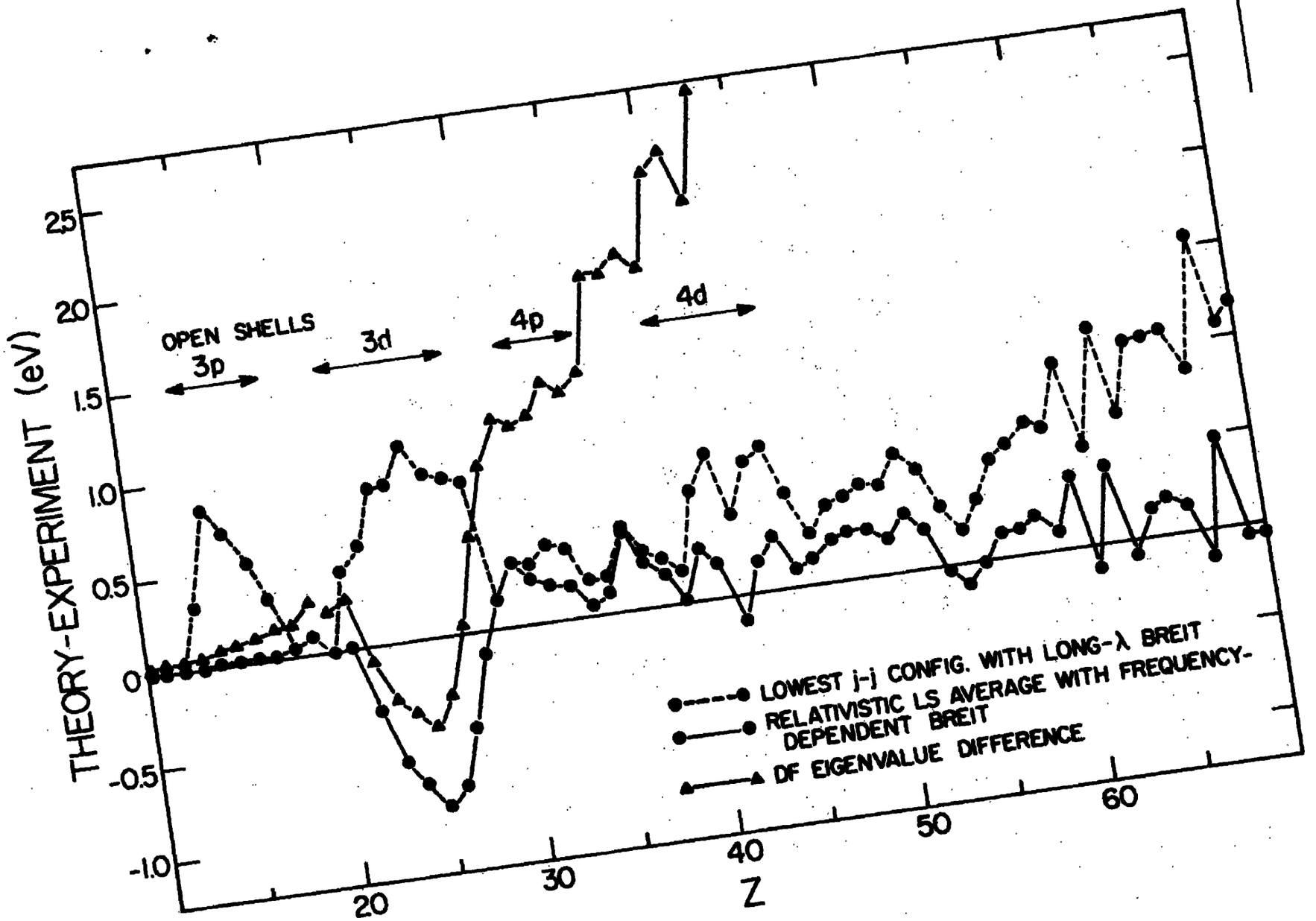
THEORY-EXPERIMENT (eV)
25
20
1.5
1.0
0.5
0
-0.5
-1.0
OPEN SHELLS
3p
3d
4p
4d
20
30
40
50
60
Z
LOWEST j-j CONFIG. WITH LONG-λ BREIT
RELATIVISTIC LS AVERAGE WITH FREQUENCY-DEPENDENT BREIT
DF EIGENVALUE DIFFERENCE

Figure 1.

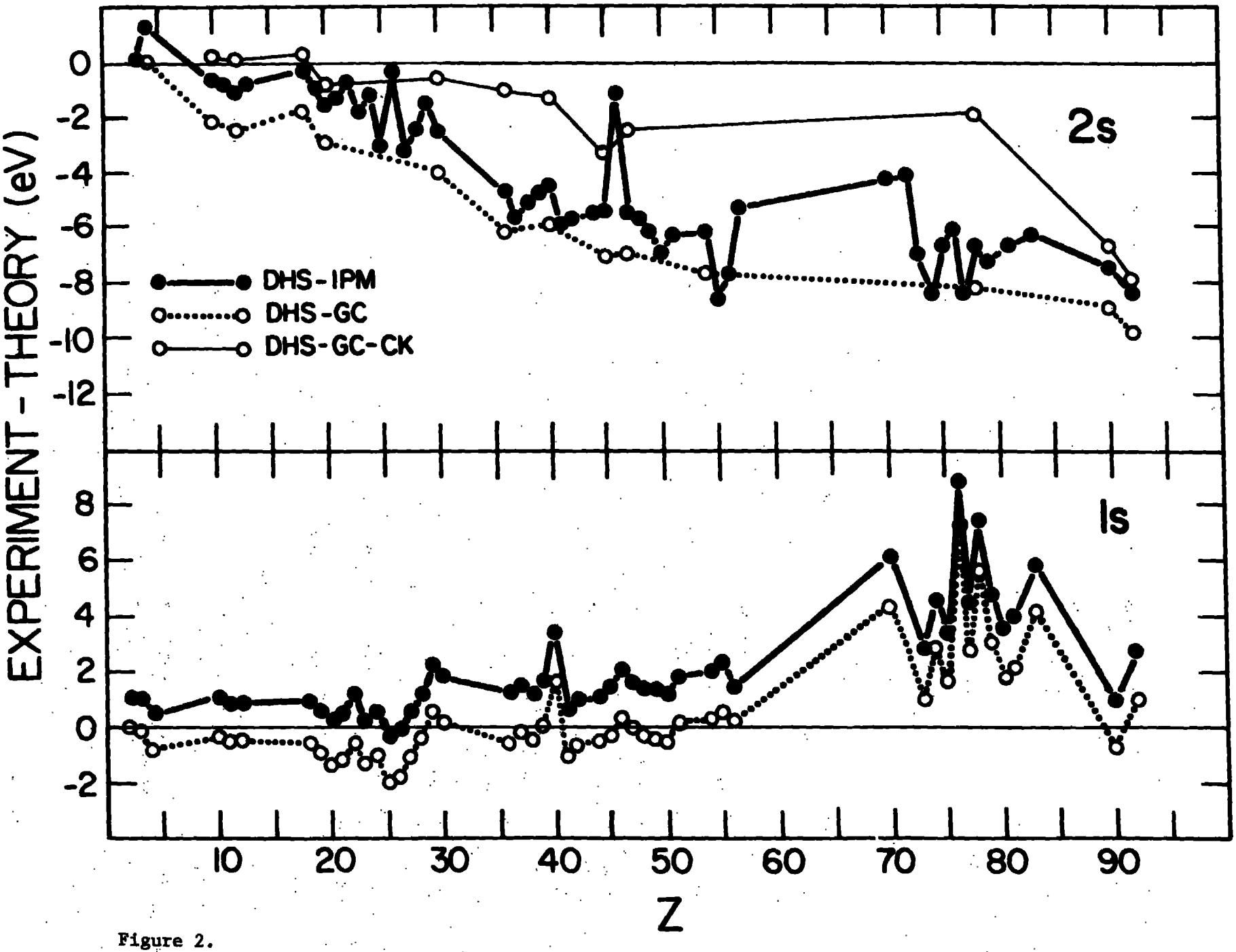
EXPERIMENT - THEORY (eV)
0
-2
-4
-6
-8
-10
-12
2s
DHS-IPM
DHS-GC
DHS-GC-CK
8
6
4
2
0
-2
1s
10
20
30
40
50
60
70
80
90
Z

Figure 2.

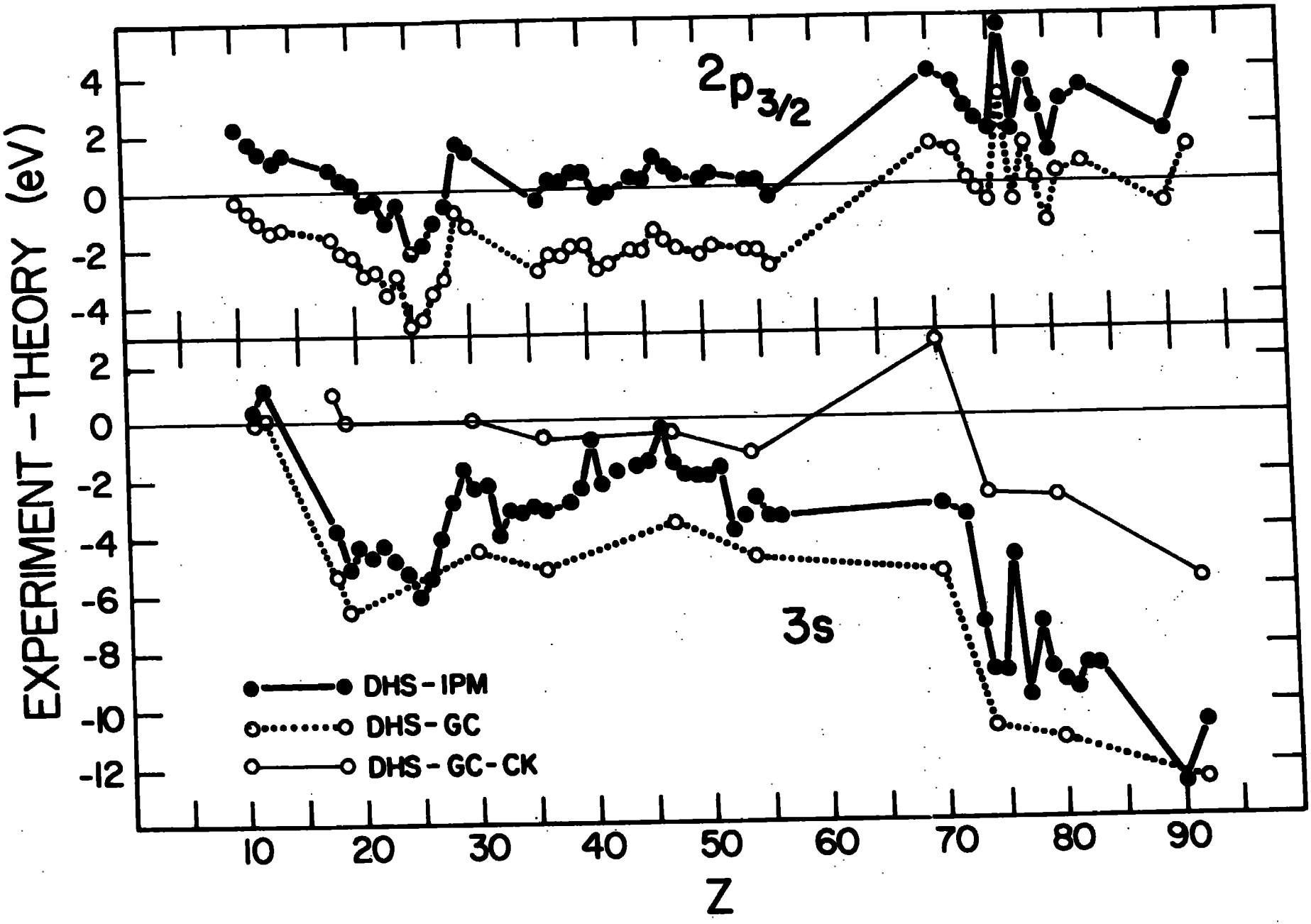
EXPERIMENT - THEORY (eV)
4
2
0
-2
-4
2
0
-2
-4
-6
-8
-10
-12
$2p_{3/2}$
3s
DHS - IPM
DHS - GC
DHS - GC - CK
10
20
30
40
50
60
70
80
90
Z

Figure 3.

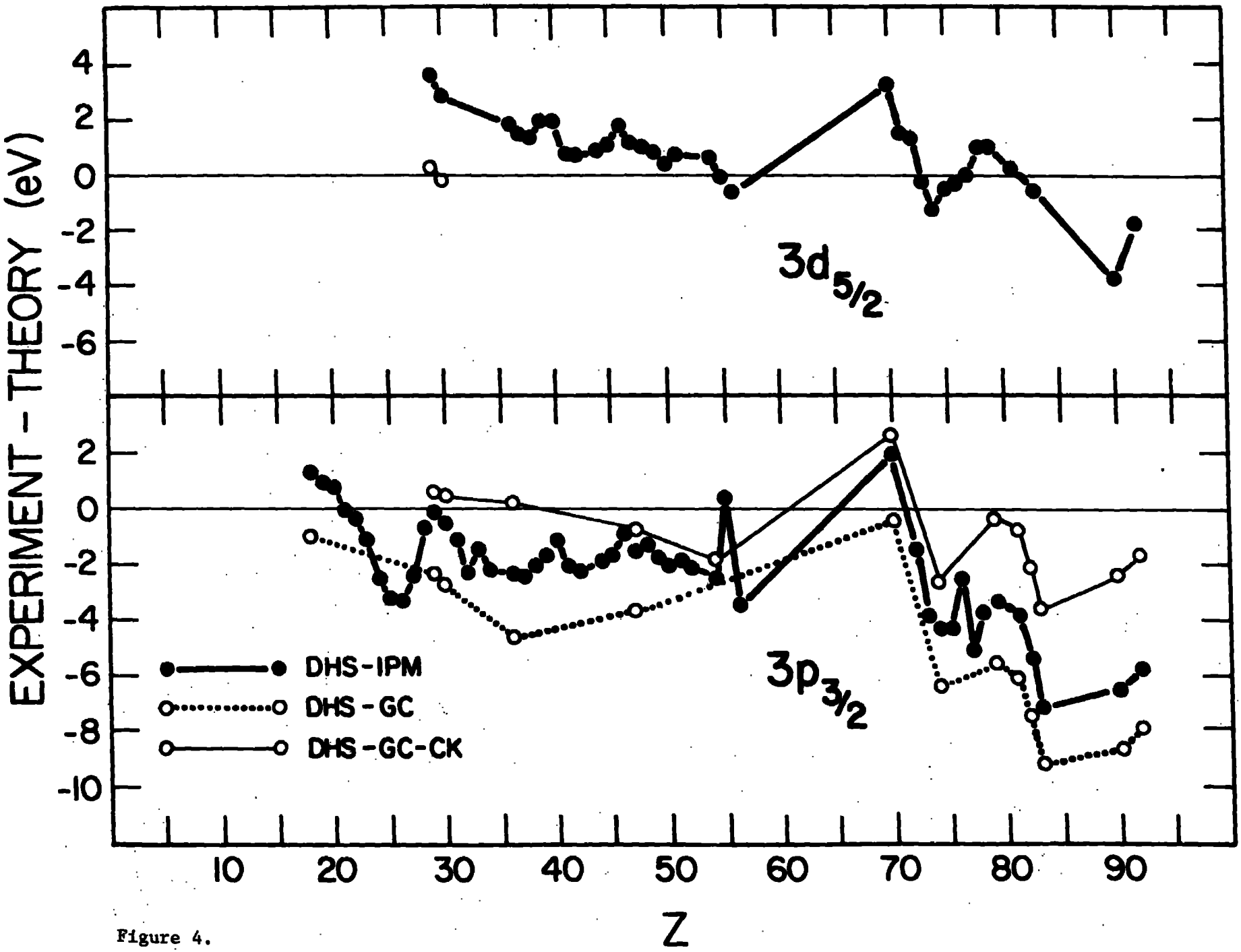
EXPERIMENT - THEORY (eV)
4
2
0
-2
-4
-6
$3d_{5/2}$
2
0
-2
-4
-6
-8
-10
$3p_{3/2}$
DHS-IPM
DHS-GC
DHS-GC-CK
10
20
30
40
50
60
70
80
90
Z

Figure 4.

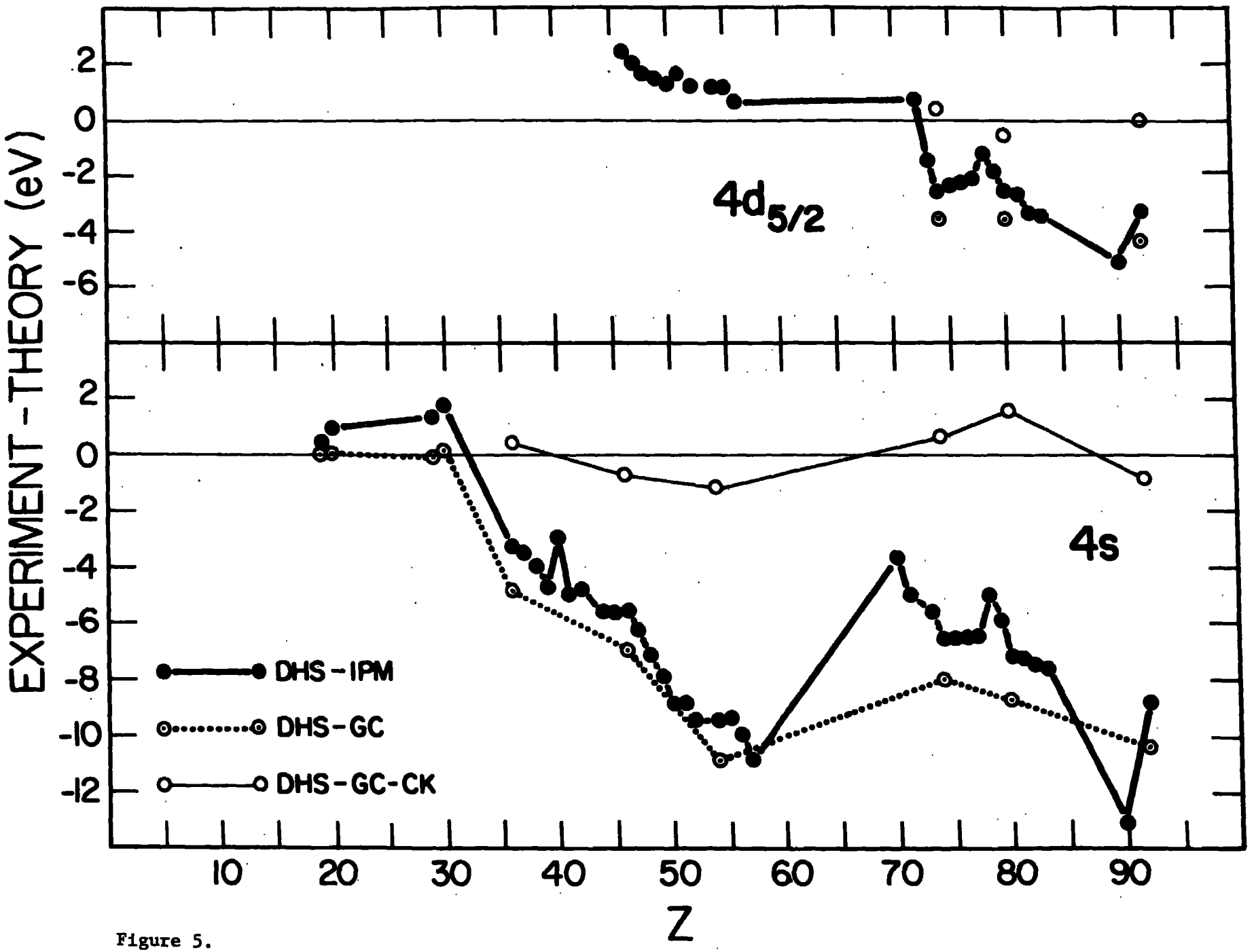
EXPERIMENT - THEORY (eV)
2
0
-2
-4
-6
4d5/2
2
0
-2
-4
-6
-8
-10
-12
4s
DHS - IPM
DHS - GC
DHS - GC - CK
10
20
30
40
50
60
70
80
90
Z

Figure 5.

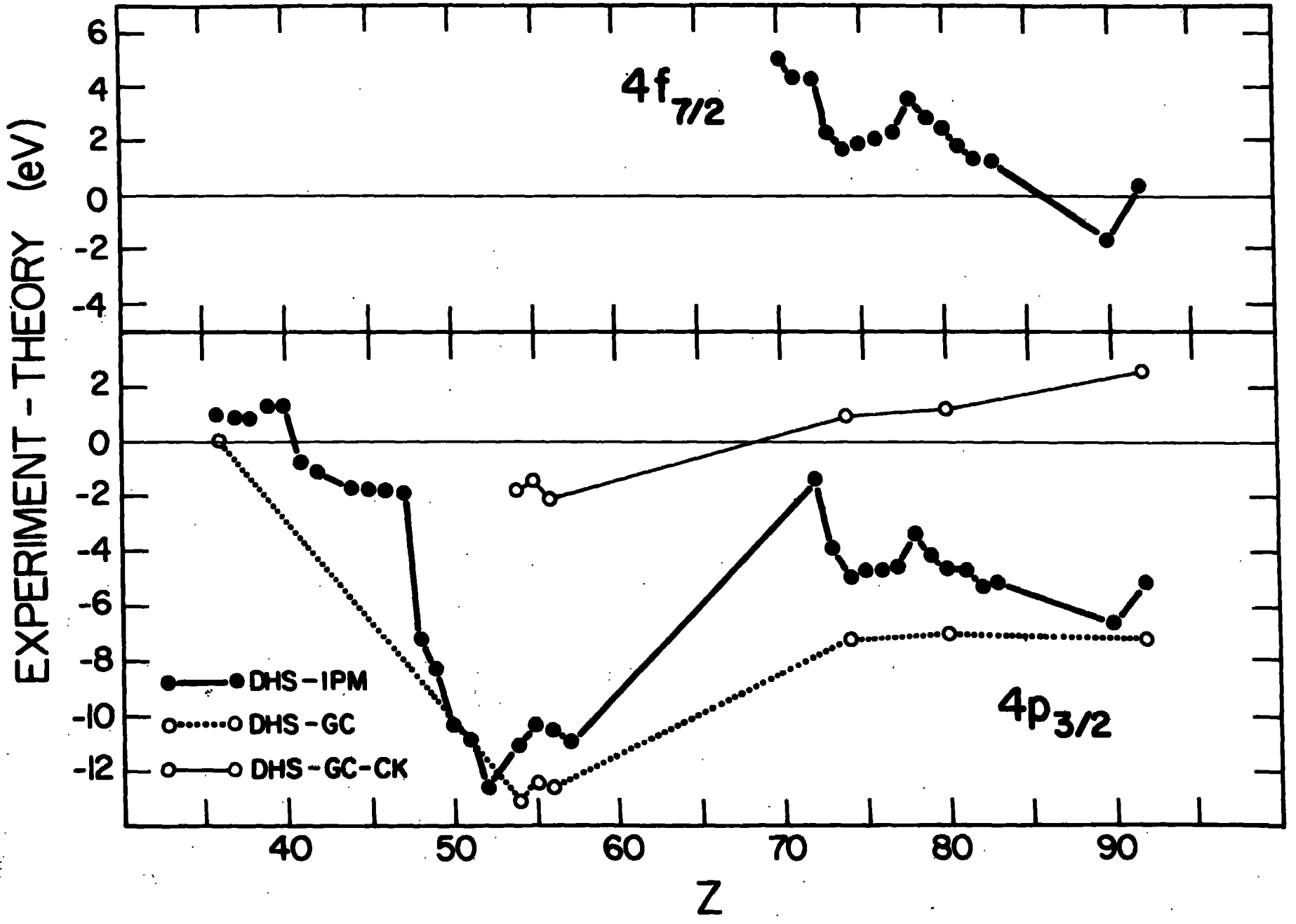
EXPERIMENT - THEORY (eV)
6
4
2
0
-2
-4
2
0
-2
-4
-6
-8
-10
-12
$4f_{7/2}$
$4p_{3/2}$
DHS - IPM
DHS - GC
DHS - GC - CK
40
50
60
70
80
90
Z

Figure 6.